original report

Majority of *B2M*-Mutant and -Deficient Colorectal Carcinomas Achieve Clinical Benefit From Immune Checkpoint Inhibitor Therapy and Are Microsatellite Instability-High

Sumit Middha, PhD[1]; Rona Yaeger, MD[1]; Jinru Shia, MD[1]; Zsofia K. Stadler, MD[1]; Sarah King[1]; Shanna Guercio[1]; Victoriya Paroder, MD[1]; David D.B. Bates, MD[1]; Satshil Rana, MS[1]; Luis A. Diaz Jr, MD[1]; Leonard Saltz, MD[1]; Neil Segal, MD[1]; Marc Ladanyi, MD[1]; Ahmet Zehir, PhD[1]; and Jaclyn F. Hechtman, MD[1]

abstract

PURPOSE Microsatellite instability-high (MSI-H) colorectal carcinomas (CRCs) show high rates of response to immune checkpoint inhibitors (IOs). *B2M* mutations and protein loss have been proposed as causes of resistance to IOs, yet they are enriched in MSI-H CRC. We aimed to characterize *B2M*-mutant, IO-naive CRC.

PATIENTS AND METHODS All CRCs with results for Memorial Sloan Kettering Integrated Mutation Profiling of Actionable Cancer Targets, a next-generation sequencing assay that interrogates > 400 genes for mutations as well as MSI status, were surveyed for *B2M* mutations. All *B2M*-mutant CRCs were assessed for expression of *B2M*, major histocompatibility complex class I, and programmed death-1 ligand (PD-L1) via immunohisto-chemistry and average CD3$^+$ and CD8$^+$ tumor-infiltrating lymphocyte counts against a control group of MSI-H *B2M* wild-type CRCs.

RESULTS Fifty-nine (3.4%) of 1,751 patients with CRC harbored *B2M* mutations, with 84% (77 of 92) of the mutations predicted to be truncating. *B2M* mutations were significantly enriched in MSI-H CRCs, with 44 (24%) of 182 MSI-H CRCs harboring *B2M* mutations (*P* < .001). Thirty-two of 44 *B2M*-mutant CRCs with available material (73%) had complete loss of *B2M* expression, whereas all 26 CRCs with wild-type *B2M* retained expression (*P* < .001). *B2M* mutation status was not associated with major histocompatibility complex class I expression, *KRAS* or *BRAF* mutation, tumor-infiltrating lymphocyte level, or PD-L1 expression after adjustment for MSI status. Of 13 patients with *B2M*-mutant CRC who received programmed death-1 or PD-L1 IOs, 11 (85%) achieved clinical benefit, defined as stable disease or partial response using Response Evaluation Criteria in Solid Tumors criteria.

CONCLUSION *B2M* mutations occur in approximately 24% of MSI-H CRCs and are usually associated with loss of *B2M* expression. Most patients with *B2M*-mutant MSI-H CRC with loss of protein expression obtain clinical benefit from IOs.

JCO Precis Oncol. © 2019 by American Society of Clinical Oncology

INTRODUCTION

The *B2M* gene encodes the protein β$_2$-microglobulin, an extracellular component of major histocompatibility complex (MHC) class I molecules that is present on every nucleated cell in the human body. MHC class I molecules are important for immune system self-recognition. B2M-deficient mice have decreased CD8$^+$ lymphocytes and are susceptible to intracellular pathogens.[1,2] With regard to cancer, acquired *B2M* mutations and loss of *B2M* expression have been implicated as causes of acquired resistance to immunotherapy in melanoma.[3] *B2M* mutations in immunotherapy-naive colorectal carcinoma (CRC) have recently been implicated as a cause of primary resistance in this disease.[4,5]

Recently, microsatellite instability-high (MSI-H) CRC has been found to have both high rates of response to immunotherapy[6-9] and, interestingly, frequent trun-cating *B2M* mutations.[10] Here, we sought to define the relationship of *B2M* mutations in CRC with expression of *B2M* and MHC class I expression, immunotherapy response, tumor-infiltrating lymphocytes (TILs), and molecular correlates.

PATIENTS AND METHODS

Molecular Analysis

Patients with CRC whose tumors were analyzed using the Memorial Sloan Kettering Integrated Mutation Profiling of Actionable Cancer Targets (MSK-IMPACT) assay (a clinically validated, US Food and Drug

CONTEXT

Do *B2M*-mutant and deficient colorectal carcinomas (CRCs) respond to immune checkpoint inhibitors?

We found that *B2M* mutations are enriched in microsatellite instability-high CRC, that these mutations commonly occur at coding microsatellite loci, and that these *B2M* mutations are truncating and associated with loss of *B2M* expression. Of 13 patients with *B2M*-mutant CRC and available RECIST data, six achieved stable disease, five achieved partial response, and one experienced pseudoprogression.

B2M mutations are not predictive of primary resistance to immune checkpoint inhibition in CRC.

Administration–cleared, next-generation sequencing assay that interrogates > 400 genes for mutations, copy-number changes, structural variants, and MSI[11-13] between January 1, 2014, and October 31, 2017, were included for *B2M*, programmed death-1 ligand (PD-L1), MHC, CD3, and CD8 immunohistochemistry (IHC) and molecular analyses. Nonsilent mutations in all coding regions as well as intronic mutations that might disrupt splice sites (up to two base pairs after exon-intron boundary) in *B2M* were recorded. Presence of loss of heterozygosity (LOH) was assessed via allele-specific copy-number analysis using the Fraction and Allele-Specific Copy Number Estimates from Tumor Sequencing (FACETS) algorithm[14] and, in cases of low tumor content, via comparison of *B2M* mutation variant allele frequency against median variant allele frequency. Clonality of *B2M* mutations was assessed by calculating the cancer-cell fraction harboring the mutations using FACETS.[14] *B2M*-mutated patient cases were considered clonal if the upper bound of the cancer-cell fraction was > 0.8. Clinical parameters, including primate site (right, cecum to splenic flexure; left, descending colon to rectum), stage at diagnosis, date of distant metastasis, and overall survival (OS), were recorded.

Clinical Response to Immune Checkpoint Inhibitor Therapy

All patients with CRC with MSK-IMPACT data and *B2M* mutations who underwent therapy with immune checkpoint inhibitors (IOs; durvalumab, nivolumab, or pembrolizumab) before July 2018 were assessed for *B2M* expression (IHC), response, stable disease (SD), and progressive disease (PD). IOs were administered as standard treatment, in clinical trials, or off label. Formal Response Evaluation Criteria in Solid Tumors (RECIST) scores were assessed via radiologic data as follows: complete response (CR), disappearance of all target lesions, confirmed at 4 weeks; partial response (PR), ≥ 30% decrease, confirmed at 4 weeks; PD, ≥ 20% increase over smallest sum observed; and SD, meeting none of the other criteria. Patients were deemed to have experienced clinical benefit from IOs if RECIST results were SD, PR, or CR.

IHC

IHC staining for *B2M* using a polyclonal antibody with concentration of 1:6,000 (catalog #A0072; Dako, Santa Clara, CA), MHC class I using a monoclonal antibody with concentration of 1:200 (catalog #14-9958; E-Bioscience, Carlsbad, CA), CD3 using a monoclonal antibody with concentration of 1:200 (catalog #NCL-L-CD3-565; Leica, Lincolnshire, IL), CD8 using a monoclonal antibody with concentration of 1:100 (catalog #M7103; Dako), and PD-L1 using a monoclonal antibody with concentration of 1:100 (catalog #13684; Cell Signaling, Danvers, MA) was performed on all CRCs with *B2M* mutations with available tissue as well as a set of 26 randomly selected wild-type (WT) CRCs with in-house resection specimens and MSK-IMPACT testing (performed between January 1, 2014, and October 31, 2017) that were matched to the *B2M*-mutant group for prevalence of MSI status. Levels of CD3+ and CD8+ TILs were assessed via the average of five counted fields per patient case at ×400 original magnification on light microscopy. IHC-positive cells were counted up to a maximum of 150 cells, because counts > 150 per high-powered field (HPF) tended to have clustering, which led to difficulty establishing accurate counts. *B2M* and MHC class I expression were each recorded as retained or lost for each patient case. Complete loss of *B2M* on IHC (0% of tumor cells with *B2M* expression) was interpreted as loss of *B2M* expression.

Statistical Analyses

Associations were assessed using Pearson's χ^2 test with simulated *P* value based on 2,000 replicates for low count data. A Cox proportional hazards model was fitted to the data to calculate survival using the covariates of *B2M* mutation status, age at diagnosis, pathologic stage, MSI status, proximal versus distal status, and *KRAS*, *NRAS*, *BRAF*, and *PIK3CA* mutation status. These were each assessed through both univariable and multivariable Cox regressions. R survival and survminer software packages were used to perform this analysis (R Foundation, Vienna, Austria).

RESULTS

Molecular Findings

We first sought to determine the spectrum of *B2M* mutations in a cohort of patients with CRC (n = 1,751) with MSK-IMPACT data (Appendix Fig A1). We identified a total of 59 patients with *B2M*-mutant CRC (3.4%; Fig 1A).

Although most *B2M* mutations were spread throughout the gene, four positions were recurrently altered (Fig 1A): p. L15Ffs*41 (CT dinucleotide repeat ×4), p. X23_splice (c. 68-2A>G), p. V69Wfs*34 (A mononucleotide repeat ×5), and p. T93Hfs*2/Lfs*10 (C mononucleotide repeat ×5). Three of these four hotspots occurred at coding microsatellites (Fig 1A). Next, we classified the samples on the basis of whether they were microsatellite stable (MSS) or unstable (MSI-H) on the basis of genomic data. We identified 182 patients who were MSI-H and 1,569 who were MSS in the overall CRC cohort. Within the MSI-H group, 44 (24.2%) harbored *B2M* mutations, whereas only 15 (0.9%) of those with MSS CRC harbored *B2M*

mutations, indicating that *B2M* mutations were significantly enriched in MSI-H CRC (*P* < .001) even after correcting for differences in total mutation counts in MSI-H versus MSS patient cases. Furthermore, of 8,790 coding microsatellites interrogated within the MSK-IMPACT panel, the *B2M* p. L15 and p. V69 microsatellites were respectively the ninth and 16th most frequently mutated coding microsatellites in MSI-H CRC. Within the 44 MSI-H *B2M*-mutant samples, we identified a total of 69 mutations, 61 (88.4%) of which were predicted to be truncating (including frameshift, splicing, and stop-gain events), compared with 16 of the 23 *B2M* mutations in MSS patient cases (69.6%; *P* = .03). Of 92 total *B2M* mutations, 49 were frameshift, 16
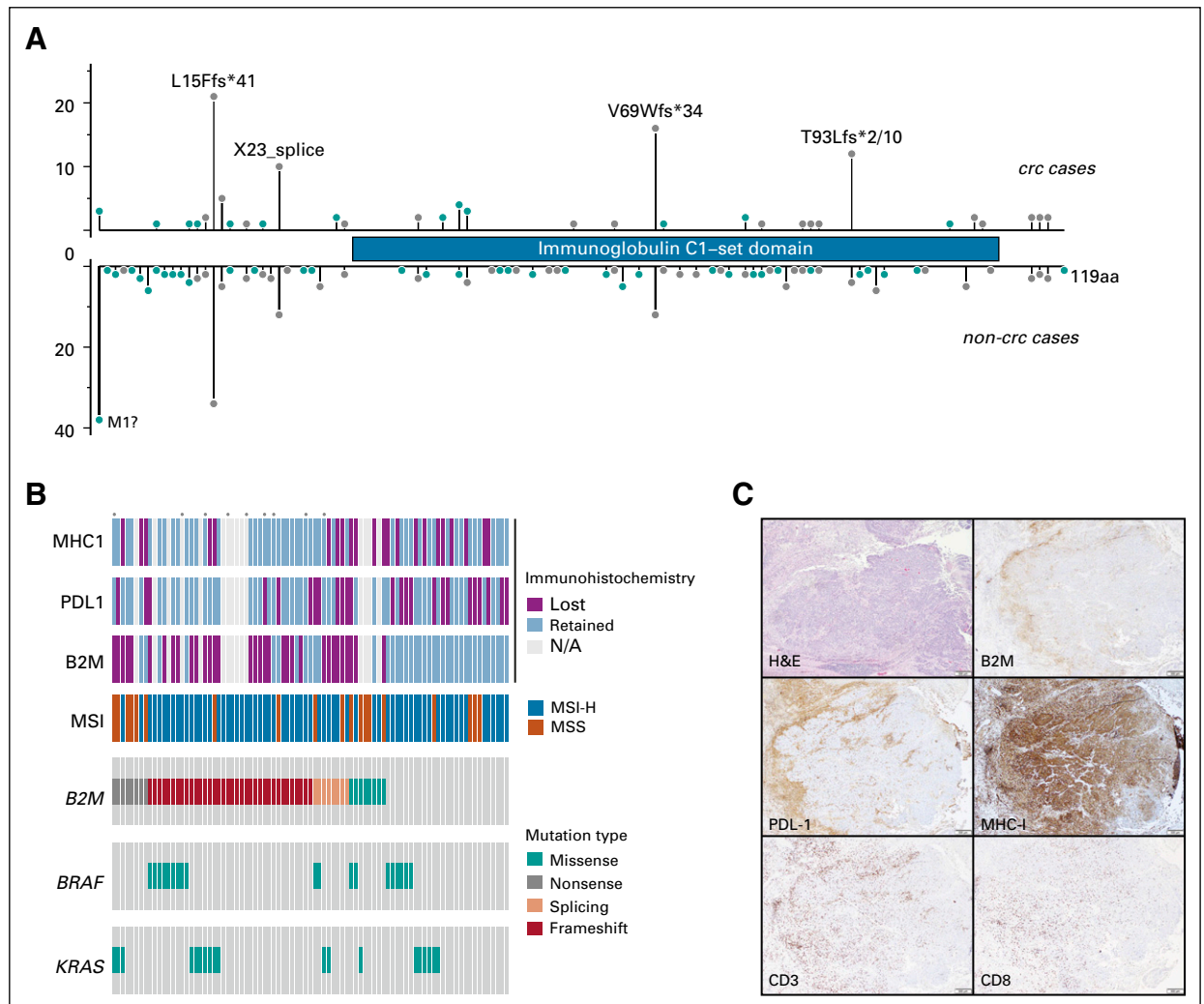

FIG 1. Spectrum of *B2M* mutations and expression. (A) Fifty-nine patients with colorectal cancer (CRC) harbored *B2M* mutations. Although several scattered missense (green) mutations were seen, truncating (gray) mutations were more frequent at several hotspots. These included microsatellite loci: 21 mutations at p. L15Ffs*41, 16 at p. V69Wfs*34, 11 at p.T93Hfs*2/Lfs*10, and 10 at the splice site p.X23. (B) Oncoprint summarizing the immunopathologic data with genomic information. Each dot above the sample indicates the patient was treated with a checkpoint inhibitor. (C) Loss of B2M expression and retained major histocompatibility complex (MHC) class I expression in a microsatellite instability-high *B2M* double-mutant (p. V69Wfs*34, p. S16Afs*27) CRC with high tumor-infiltrating lymphocyte level. A medullary carcinoma of the colon shows immune-cell expression of programmed death-1 ligand at the tumor-stroma interface, loss of B2M expression in tumor cells, retention of strong diffuse MHC class I expression in tumor cells, > 150 CD3+ lymphocytes per high-powered field (HPF), and average of 69 CD8+ cells per HPF.

were nonsense, 15 were missense, nine were splice-site, and three were translation initiation codon mutations. *KRAS* and *BRAF* p. V600E mutations were not significantly associated with *B2M* mutation status after adjustment for MSI status (Table 1).

We performed allele-specific copy-number analysis on 45 *B2M*-mutant specimens where sufficient tumor content was available. Forty-one of 45 *B2M*-mutant CRCs had at least one clonal *B2M* mutation on the basis of FACETS analysis (12 samples with one clonal mutation and 29 with > one; Appendix Table A1). Twelve samples showed either LOH or copy-neutral LOH along with a clonal mutation, suggesting biallelic loss.

B2M Expression, MHC Class I Expression, and TIL Level

To evaluate the functional outcome of *B2M* mutations, we examined protein expression in samples with available tissue (Figs 1B and 1C; Appendix Table A2). Thirty-two (73%) of 44 *B2M*-mutated CRCs with available tissue had complete loss of B2M expression, whereas the remaining 12 *B2M*-mutant CRCs had varying proportions of tumor cells expressing B2M (20%,

n = 2; 30%, n = 1; 40%, n = 1; 50%, n = 3; and 100%, n = 5). All 26 *B2M* WT CRCs retained B2M expression. Loss of B2M expression was significantly associated with *B2M* mutation in immunotherapy-naive CRC (*P* = .001).

Because *B2M* protein is an essential part of the MHC complex, we explored the effects of B2M loss on MHC class I expression. MHC class I IHC was performed in 44 *B2M*-mutated CRCs, of which only 14 (30%) had loss of MHC expression. Of the 26 *B2M* WT CRCs, 10 (39%) had MHC class I loss. MHC class I expression by IHC did not correlate with either *B2M* mutation or B2M expression. Because PD-L1 status has been used as a predictive marker of IOs and linked to expression of MHC class 1, we performed PD-L1 IHC in available *B2M*-mutant and WT patient cases. Thirty-two (73%) of 44 *B2M*-mutant and 13 (50%) of 26 *B2M* WT CRCs were positive for PD-L1 expression (immune cells in tumor-stroma interface). The difference in PD-L1 expression between the two groups did not reach statistical significance (*P* = .07).

TIL level has been directly correlated with prognosis and implicated as a marker of neoantigen level and potential

TABLE 1. Clinical and Molecular Characteristics of *B2M* Mutations in CRC

Characteristic	*B2M* Mutated (n = 59)	*B2M* WT (n = 1,762)	P
Sex			.61
Female	25 (42.4)	801 (45.5)	
Male	34 (57.6)	948 (53.8)	
Not specified	0 (0)	13 (0.7)	
Age at diagnosis of metastasis, years			.76
Median	58.3	55.3	
Mean	55.9	55.5	
Stage			< .001
I	5 (8.5)	63 (3.6)	
II	18 (30.5)	196 (11.1)	
III	21 (35.6)	393 (22.3)	
IV	13 (22)	1001 56.8)	
Unknown	2 (3.4)	109 (37.2)	
Stage (I-III *v* IV)			< .001
Late (IV)	13 (22)	1001 (56.8)	
Early (I, II or III)	44 (74.6)	654 (37.1)	
MSI status			< .001
MSI-H (score ≥ 10)	44 (74.6)	141 (8)	
MSS (score < 10)	15 (25.4)	1621 (92)	
KRAS/BRAF mutations			.26*
KRAS	25 (42.4)	744 (42.2)	
BRAF p. V600E	13 (22)	126 (7.2)	

Abbreviations: CRC, colorectal cancer; MSI, microsatellite instability; MSI-H, MSI-high; MSS, microsatellite stable; WT, wild type.

*P = .82 after adjustment for MSI status.

immunotherapy response.[15] We examined the number of TILs using the pan–T-cell marker CD3 and the cytotoxic T-cell marker CD8. Average median CD3$^+$ count per HPF was 22.3 in *B2M*-mutant and 37.3 in *B2M* WT CRCs, whereas average median CD8$^+$ count per HPF was 15.1 and 49 for *B2M*-mutant and *B2M* WT CRCs, respectively. In comparison with *B2M* WT CRCs matched for MSI status, *B2M*-mutant CRCs tended to have lower average levels of CD3 and CD8 per patient case (Fig 2A), but these differences did not reach statistical significance. These findings are summarized in Appendix Table A2.

Clinical Findings

Median age, male-to-female ratio, and percentage of patients with early-stage (stage I to III) disease were 58.3 years, 1.36, and 77.19% in *B2M*-mutant and 55.3 years, 1.18, and 39.52% in *B2M* WT CRCs, respectively. On multivariable analysis, *B2M* mutation status was not associated with OS from date of metastasis ($P = .90$). Age, stage, and *KRAS*, *NRAS*, and *BRAF* status were associated with OS, whereas *PIK3CA* mutation status, MSI status, and proximal versus distal location were not associated with OS (Fig 2B; Appendix Table A2).

Response to Immunotherapy

Because *B2M* mutations were identified as a possible resistance mechanism for checkpoint inhibition, we identified 13 (MSI-H, n = 11; MSS, n = 2) patients with CRC with *B2M* mutations who subsequently received IO therapy, and we evaluated their response to treatment. This group of patients predominantly consisted of those with MSI-H

FIG 2. Comparison of tumor-infiltrating lymphocyte (TIL) levels and predictors of overall survival (OS). (A) Box plot graphs of average CD3 (left) and CD8 (right) counts in *B2M*-mutant vs wild-type (WT) colorectal carcinoma (CRC) show that median average CD3 and CD8 trend toward higher values in *B2M* WT carcinoma. (B) Multivariable model showing the clinical variables associated with OS of patients with CRC in our cohort. Error bars indicate 95% CI for hazard ratios. MSI-H, microsatellite instability-high. Asterisks indicate level of significance.
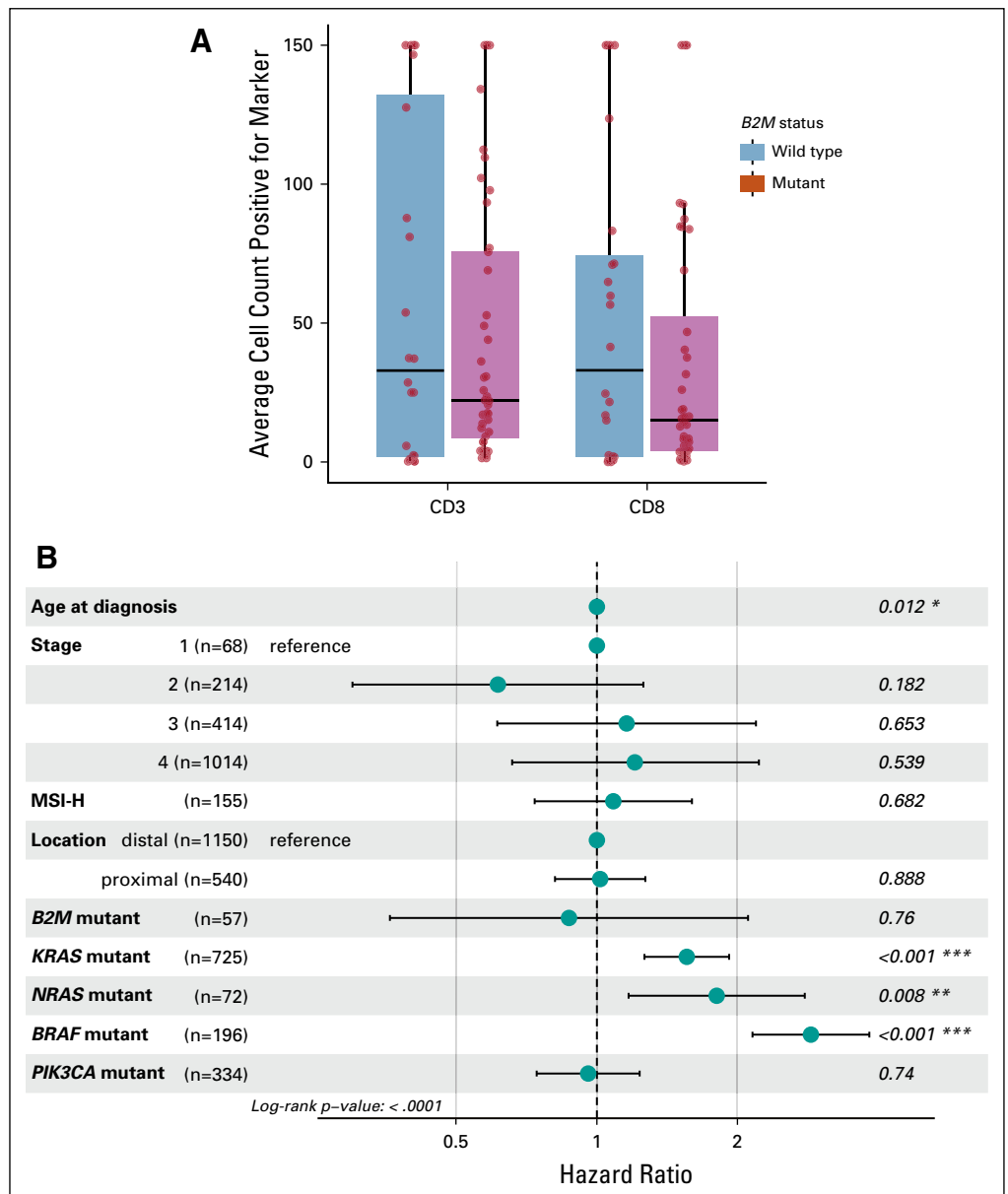
tumors but included two patients with MSS disease. One patient's tumor was hypermutated because of an exonucelase domain mutation in the *POLE* gene. IOs administered to patients included PD-L1 inhibitors (n = 3 patients) and programmed death-1 inhibitors (n = 10 patients). Because some patients received treatment in ongoing clinical trials, specific IOs are not listed. Analysis of their tumor response by RECIST criteria demonstrated PR in five patients, SD in six patients, and PD in one patient, likely pseudoprogression (Fig 3A; Appendix Table A3). *B2M* mutation was biallelic in half the patients and did not lead to a significant difference in response to treatment. One patient experienced progression without radiologic studies, and RECIST evaluation could not be completed. This response rate is in line with recent publications of IOs in MSI-H CRC.[8,9] Of the two patients with MSS tumors, one had an ultramutated *POLE* hotspot–mutated tumor and experienced tumor growth with IO treatment but was able to continue treatment for 1 year, because growth was thought likely to be pseudoprogression, and the other patient had SD during treatment with a combination of IO treatment and targeted therapy (after progression with targeted therapy alone). All patients except this MSS patient were treated with immunotherapy alone. Median treatment time was 5 months (Fig 3B); three of the 12 patients stopped treatment because of toxicity.

DISCUSSION

In this study, we show that *B2M* mutations occurred in approximately 24% of immunotherapy-naive MSI-H CRCs and were associated with B2M loss in 93% of patient cases (usually without loss of MHC class I), and 85% of *B2M*-mutant CRCs demonstrated some clinical benefit from IOs. As IO therapy becomes standard treatment in advanced MSI-H CRC, the importance of identifying additional predictors of response and resistance to checkpoint inhibitors has also grown.

Our molecular findings, including enrichment of *B2M* mutations in MSI-H CRC and *B2M* mutations occurring at certain hotspots, are consistent with previous reports. Both findings likely result from the fact that there are several coding mono- and dinucleotide microsatellites within *B2M*. In addition, *B2M* mutations may confer a growth advantage for MSI-H CRC tumors, as suggested by the facts that *B2M* mutations were statically significantly enriched in MSI-H CRC after adjustment for total mutation count and that two coding microsatellites in *B2M* are within the top 20 most frequently mutated coding microsatellites of 8,790 microsatellites assessed. That *B2M* mutations in CRC are usually associated with loss of B2M expression indicates that a second hit or LOH occurs. The association of *B2M* mutations with complete loss of expression on whole sections of

FIG 3. Immune checkpoint inhibitor (IO) response in *B2M*-mutant colorectal cancer (CRC). Waterfall plot of IO response in *B2M*-mutant CRC (colored by microsatellite instability [MSI] status, type of *B2M* mutation, and type of IO received). (B) Duration of treatment, with different colors indicating if the patient is still undergoing treatment or has stopped receiving IOs. Patient P-0025883 was not included in this graph because of nonmeasurable disease. MSI-H, MSI-high; MSS, microsatellite stable; PD-1, programmed death-1; PD-L1, PD-1 ligand.
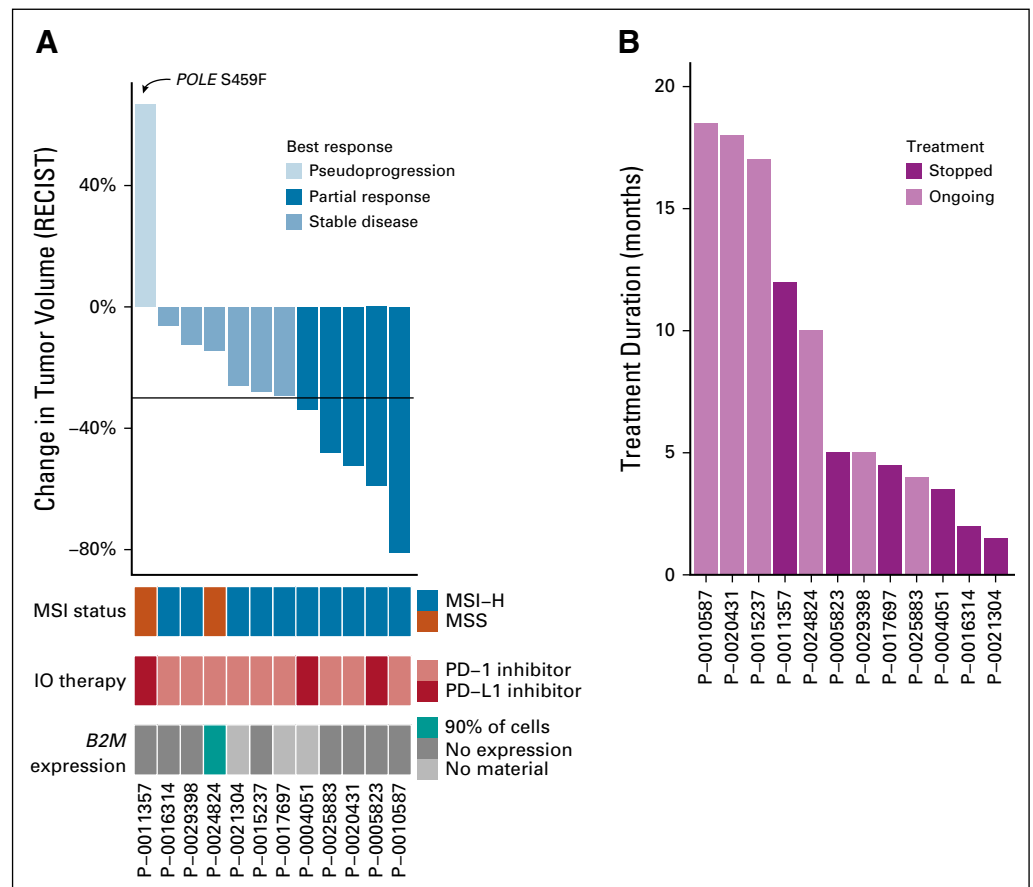
tumor also argues against the idea that mutation subclonality may be responsible for response to immunotherapy. Indeed, in the 42 *B2M*-mutant CRCs analyzed by FACETS, 60% had evidence of either two clonal *B2M* mutations or one clonal *B2M* mutation and LOH (Appendix Table A1). It is possible that the remaining *B2M*-mutant CRCs have epigenetic modifications as a mechanism of *B2M* silencing.

Unlike previous studies,[3] we found that B2M protein loss is not correlated with loss of MHC class I expression. Although previous studies have focused on patients with resistance to immunotherapy, the patients in this study were immunotherapy naive. We show that *B2M* mutation and loss do not correlate with MHC class I loss of expression, although the effect of B2M loss on the functional competence of MHC class I is known to be deleterious.[16]

Limitations to our study include the retrospective analysis and relatively small number of patients treated with IOs, as well as limitations in molecular testing for epigenetic issues and allele specificity of *B2M* mutations.

Most importantly, our study shows that *B2M* mutation and loss in immunotherapy-naive CRC do not predict primary resistance to IOs. We focused on whether patients receiving IOs can benefit from treatment if their tumors have *B2M* mutations and protein loss. We saw that most patients had some degree of regression with treatment; larger, prospective studies are needed to clarify if the response rate and duration of response vary by *B2M* mutation status. However, our data indicate that patients with CRC whose tumors harbor *B2M* mutations should not be excluded from IO treatment. Giannakis et al[15] have shown that TIL level predicts neoantigen load. The clinical benefit demonstrated in patients with B2M-deficient CRC who received IOs may have resulted from the fact that despite B2M loss, there was still evidence of functional neoantigen recognition, as indicated by the high number of TILs (median, 22.3 per HPF) still present in B2M-deficient MSI-H CRC. Thus, *B2M* loss may not be sufficient to lead to primary resistance to immunotherapy in MSI-H CRC.

AFFILIATION
[1]Memorial Sloan Kettering Cancer Center, New York, NY

CORRESPONDING AUTHOR
Jaclyn F. Hechtman, MD, Memorial Sloan Kettering Cancer Center, 1275 York Ave, New York, NY 10065; Twitter: @JackieHechtman, @sloan_kettering; e-mail: hechtmaj@mskcc.org.

EQUAL CONTRIBUTION
A.Z. and J.F.H. contributed equally to this work.

AUTHOR CONTRIBUTIONS
Conception and design: Sumit Middha, Marc Ladanyi, Ahmet Zehir, Jaclyn F. Hechtman
Collection and assembly of data: Sumit Middha, Rona Yaeger, Jinru Shia, Sarah King, Shanna Guercio, Victoriya Paroder, David D.B. Bates, Neil Segal, Ahmet Zehir, Jaclyn F. Hechtman
Data analysis and interpretation: Sumit Middha, Rona Yaeger, Jinru Shia, Zsofia K. Stadler, Victoriya Paroder, Satshil Rana, Luis A. Diaz Jr, Leonard Saltz, Marc Ladanyi, Ahmet Zehir, Jaclyn F. Hechtman
Manuscript writing: All authors
Final approval of manuscript: All authors

AUTHORS' DISCLOSURES OF POTENTIAL CONFLICTS OF INTEREST AND DATA AVAILABILITY STATEMENT
The following represents disclosure information provided by authors of this manuscript. All relationships are considered compensated. Relationships are self-held unless noted. I = Immediate Family Member, Inst = My Institution. Relationships may not relate to the subject matter of this manuscript. For more information about ASCO's conflict of interest policy, please refer to www.asco.org/rwc or ascopubs.org/po/author-center.

Rona Yaeger
Research Funding: Array BioPharma, GlaxoSmithKline, Novartis
Travel, Accommodations, Expenses: Array BioPharma

Zsofia K. Stadler
Consulting or Advisory Role: Allergan (I), Genentech/Roche (I), Regeneron (I), Optos (I), Adverum (I), Biomarin (I), Alimera Sciences (I), Novartis (I), Spark Therapeutics (I), Fortress Biotech (I), Regenxbio (I)

Luis A. Diaz Jr
Leadership: Personal Genome Diagnostics, Jounce Therapeutics
Stock and Other Ownership Interests: PapGene, Personal Genome Diagnostics, Jounce Therapeutics, Zydecom
Consulting or Advisory Role: Merck, Personal Genome Diagnostics, Cell Design Labs, Phoremost, Lyndra, Caris Life Sciences, Genocea Biosciences, Zydecom
Research Funding: Merck (Inst)
Patents, Royalties, Other Intellectual Property: US-2010041048-A1 Circulating mutant DNA to assess tumor dynamics; US-2015344970-A1 personalized tumor biomarkers; WO-2010118016-A2 digital quantification of DNA methylation; US-2005202465-A1 thymidylate synthase gene and metastasis; US-2014227271-A1 somatic mutations in *ATRX* in brain cancer; WO-2012094401-A2 genes frequently altered in pancreatic neuroendocrine tumors; US-2013323167-A1 detecting and treating solid tumors through selective disruption of tumor vasculature; EP-2912468-B1 Papanicolaou test for ovarian and endometrial cancers; US-9976184-B2 mutations in pancreatic neoplasms; US-2017267760-A1 checkpoint blockade and microsatellite instability; US-2018171413-A1 head and neck squamous cell carcinoma assays; US-2018086832-A1 HLA-restricted epitopes encoded by somatically mutated genes; US-2018258490-A1 assaying ovarian cyst fluid; US-2016208340-A1 TERT promoter mutations in urothelial neoplasia; US-2015252415-A1 Arid1b and neuroblastoma; WO-2018071796-A2 compositions and methods for identifying functional antitumor T-cell responses; EP-3322824-A1 detection of tumor-derived DNA in cerebrospinal fluid; US-2016273049-A1 systems and methods for analyzing nucleic acid (Inst); US-2018135044-A1 nonunique barcodes in a genotyping assay (Inst); US-2017016075-A1 neoantigen analysis (Inst)
Travel, Accommodations, Expenses: Merck

REFERENCES

1. Roberts AD, Ordway DJ, Orme IM: *Listeria monocytogenes* infection in beta 2 microglobulin-deficient mice. Infect Immun 61:1113-1116, 1993

2. Schaible UE, Collins HL, Priem F, et al: Correction of the iron overload defect in beta-2-microglobulin knockout mice by lactoferrin abolishes their increased susceptibility to tuberculosis. J Exp Med 196:1507-1513, 2002

3. Sade-Feldman M, Jiao YJ, Chen JH, et al: Resistance to checkpoint blockade therapy through inactivation of antigen presentation. Nat Commun 8:1136, 2017

4. Janikovits J, Müller M, Krzykalla J, et al: High numbers of PDCD1 (PD-1)-positive T cells and *B2M* mutations in microsatellite-unstable colorectal cancer. OncoImmunology 7:e1390640, 2017

5. Grasso CS, Giannakis M, Wells DK, et al: Genetic mechanisms of immune evasion in colorectal cancer. Cancer Discov 8:730-749, 2018

6. Le DT, Uram JN, Wang H, et al: PD-1 blockade in tumors with mismatch-repair deficiency. N Engl J Med 372:2509-2520, 2015

7. Riaz N, Havel JJ, Makarov V, et al: Tumor and microenvironment evolution during immunotherapy with nivolumab. Cell 171:934-949.e16, 2017

8. Le DT, Durham JN, Smith KN, et al: Mismatch repair deficiency predicts response of solid tumors to PD-1 blockade. Science 357:409-413, 2017

9. Overman MJ, McDermott R, Leach JL, et al: Nivolumab in patients with metastatic DNA mismatch repair-deficient or microsatellite instability-high colorectal cancer (CheckMate 142): An open-label, multicentre, phase 2 study. Lancet Oncol 18:1182-1191, 2017

10. Clendenning M, Huang A, Jayasekara H, et al: Somatic mutations of the coding microsatellites within the beta-2-microglobulin gene in mismatch repair-deficient colorectal cancers and adenomas. Fam Cancer 17:91-100, 2018

11. Zehir A, Benayed R, Shah RH, et al: Mutational landscape of metastatic cancer revealed from prospective clinical sequencing of 10,000 patients. Nat Med 23:703-713, 2017

12. Cheng DT, Mitchell TN, Zehir A, et al: Memorial Sloan Kettering-Integrated Mutation Profiling of Actionable Cancer Targets (MSK-IMPACT): A hybridization capture-based next-generation sequencing clinical assay for solid tumor molecular oncology. J Mol Diagn 17:251-264, 2015

13. Middha S, Zhang L, Naka K et al: Reliable pan-cancer microsatellite instability assessment by using targeted next-generation sequencing data. JCO Precis Oncol 10.1200/PO.17.00084, 2017

14. Shen R, Seshan VE: FACETS: allele-specific copy number and clonal heterogeneity analysis tool for high-throughput DNA sequencing. Nucleic Acids Res 44:e131, 2016

15. Giannakis M, Mu XJ, Shukla SA, et al: Genomic correlates of immune-cell infiltrates in colorectal carcinoma. Cell Reports 15:857-865, 2016 [Erratum: Cell Rep 17:1206, 2016]

16. Hulpke S, Tampé R: The MHC I loading complex: A multitasking machinery in adaptive immunity. Trends Biochem Sci 38:412-420, 2013

∎∎∎

APPENDIX

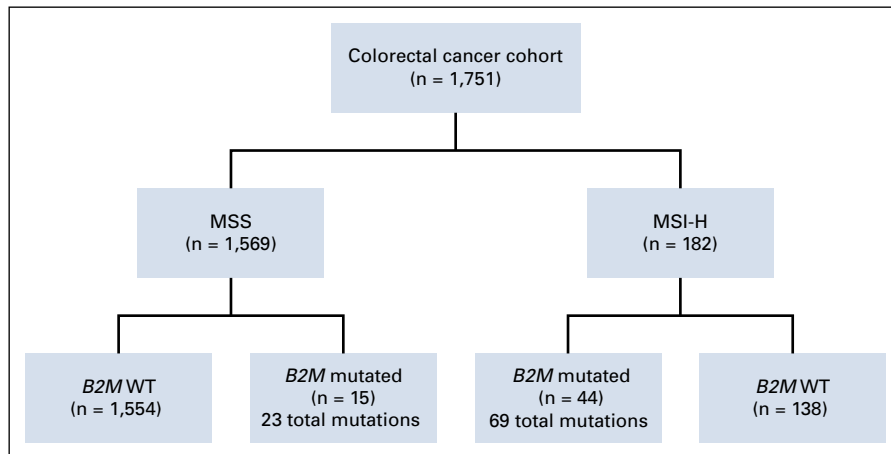**FIG A1.** CONSORT diagram. Mutation and immunohistochemistry analyses included data from 1,751 patients with colorectal cancer (CRC) with Memorial Sloan Kettering Integrated Mutation Profiling of Actionable Cancer Targets testing. Fifteen of 1,569 microsatellite stable (MSS) CRCs harbored *B2M* mutations, whereas 138 of 182 microsatellite instability-high (MSI-H) CRCs harbored *B2M* mutations. WT, wild type.

TABLE A1. Predicted *B2M* Mutation Clonality by Cellularity-Corrected Allele Fraction via FACETS and Corresponding Protein Expression (IHC)

Sample ID	Protein Change	Mutation Type	CCF	CCF Lower Bound	CCF Upper Bound	Predicted Clonality	B2M Expression (%)	No. of Clonal *B2M* Mutations	FACETS Call	TCN	LCN
P-0010587-T01-IM5	p.V69Wfs*34	Frameshift	1.00	0.98	1.00	Clonal	0	2	DIPLOID	2	1
P-0010587-T01-IM5	p.L15Ffs*41	Frameshift	1.00	0.99	1.00	Clonal	0	2	DIPLOID	2	1
P-0005823-T01-IM5	p.V69Wfs*34	Frameshift	1.00	0.98	1.00	Clonal	20	2	DIPLOID	2	1
P-0005823-T01-IM5	p.T93Lfs*10	Frameshift	0.95	0.89	1.00	Clonal	20	2	DIPLOID	2	1
P-0020431-T01-IM6	p.X116_splice	Splice donor	0.53	0.43	0.65	Subclonal	0	0	DIPLOID	2	1
P-0004051-T01-IM5	p.L15Ffs*41	Frameshift	NA	NA	NA	NA	No material	NA	DIPLOID	2	1
P-0004051-T01-IM5	p.T93Hfs*2	Frameshift	NA	NA	NA	NA	No material	NA	DIPLOID	2	1
P-0017697-T01-IM6	p.X23_splice	Splice acceptor	1.00	0.87	1.00	Clonal	No material	1	DIPLOID	2	1
P-0017697-T01-IM6	p.V69Wfs*34	Frameshift	0.71	0.63	0.79	Subclonal	No material	1	DIPLOID	2	1
P-0015237-T01-IM6	p.V69Wfs*34	Frameshift	1.00	0.99	1.00	Clonal	0	2	GAIN	4	0
P-0015237-T01-IM6	p.S16Afs*27	Frameshift	1.00	1.00	1.00	Clonal	0	2	GAIN	4	0
P-0021304-T01-IM6	p.L15Ffs*41	Frameshift	1.00	1.00	1.00	Clonal	No material	1	DIPLOID	2	1
P-0016314-T01-IM6	p.T93Hfs*2	Frameshift	0.94	0.90	0.98	Clonal	50	1	DIPLOID	2	1
P-0016314-T01-IM6	p.L15Ffs*41	Frameshift	0.32	0.29	0.35	Subclonal	50	1	DIPLOID	2	1
P-0016314-T01-IM6	p.L13P	Missense	0.61	0.56	0.65	Subclonal	50	1	DIPLOID	2	1
P-0011357-T01-IM5	p.E64*	Stop gained	0.79	0.68	0.91	Clonal	0	2	DIPLOID	2	1
P-0011357-T01-IM5	p.Y87*	Stop gained	0.80	0.69	0.92	Clonal	0	2	DIPLOID	2	1
P-0007495-T01-IM5	p.S31*	Stop gained	1.00	0.99	1.00	Clonal	0	1	CNLOH	2	0
P-0004083-T01-IM5	p.X23_splice	Splice acceptor	0.81	0.72	0.91	Clonal	0	2	DIPLOID	2	1
P-0004083-T01-IM5	p.L15Ffs*41	Frameshift	0.92	0.83	1.00	Clonal	0	2	DIPLOID	2	1
P-0004602-T01-IM5	p.L15Ffs*41	Frameshift	NA	NA	NA	NA	0	NA	DIPLOID	2	1
P-0004602-T01-IM5	p.X23_splice	Splice acceptor	NA	NA	NA	NA	0	NA	DIPLOID	2	1
P-0004738-T01-IM5	p.C45*	Stop gained	0.93	0.80	1.00	Clonal	50	1	DIPLOID	2	1
P-0005548-T01-IM5	p.T93Hfs*2	Frameshift	NA	NA	NA	NA	100	NA	LOH	1	0
P-0005443-T01-IM5	p.L15Ffs*41	Frameshift	0.98	0.87	1.00	Clonal	0	2	DIPLOID	2	1
P-0005443-T01-IM5	p.X23_splice	Splice acceptor	0.93	0.78	1.00	Clonal	0	2	DIPLOID	2	1
P-0005455-T01-IM5	p.X23_splice	Splice acceptor	1.00	0.98	1.00	Clonal	0	1	DIPLOID	2	1
P-0005529-T01-IM5	p.X23_splice	Splice acceptor	0.83	0.75	0.91	Clonal	40	2	DIPLOID	2	1
P-0005529-T01-IM5	p.C45R	Missense	0.96	0.90	1.00	Clonal	40	2	DIPLOID	2	1
P-0006681-T01-IM5	p.X115_splice	Splice donor	0.93	0.87	0.99	Clonal	0	1	LOH	1	0
P-0005824-T01-IM5	p.E70D	Missense	0.98	0.90	1.00	Clonal	0	1	DIPLOID	2	1
P-0005824-T01-IM5	p.S108*	Stop gained	0.49	0.42	0.56	Subclonal	0	1	DIPLOID	2	1
P-0006170-T01-IM5	p.W80*	Stop gained	NA	NA	NA	NA	0	NA	DIPLOID	2	1

(Continued on following page)

TABLE A1. Predicted *B2M* Mutation Clonality by Cellularity-Corrected Allele Fraction via FACETS and Corresponding Protein Expression (IHC) (Continued)

Sample ID	Protein Change	Mutation Type	CCF	CCF Lower Bound	CCF Upper Bound	Predicted Clonality	B2M Expression (%)	No. of Clonal *B2M* Mutations	FACETS Call	TCN	LCN
P-0006170-T01-IM5	p.L15Fs*41	Frameshift	NA	NA	NA	NA	0	NA	DIPLOID	2	1
P-0006612-T01-IM5	p.R117*	Stop gained	1.00	1.00	1.00	Clonal	20	1	DIPLOID	2	1
P-0007774-T01-IM5	p.L15Fs*41	Frameshift	0.80	0.76	0.85	Clonal	0	1	LOH	1	0
P-0006960-T01-IM5	p.L12P	Missense	1.00	0.95	1.00	Clonal	0	2	DIPLOID	2	1
P-0006960-T01-IM5	p.E19*	Stop gained	0.86	0.76	0.97	Clonal	0	2	DIPLOID	2	1
P-0010167-T01-IM5	p.S14Fs*29	Frameshift	0.71	0.61	0.81	Clonal	0	0	LOH	1	0
P-0013594-T01-IM5	p.L15Fs*41	Frameshift	0.16	0.14	0.19	Subclonal	100	0	LOH	1	0
P-0007836-T01-IM5	p.S16Afs*27	Frameshift	1.00	0.99	1.00	Clonal	0	2	DIPLOID	2	1
P-0007836-T01-IM5	p.Y46Cfs*10	Frameshift	1.00	0.99	1.00	Clonal	0	2	DIPLOID	2	1
P-0016181-T01-IM6	p.L59*	Frameshift	1.00	0.95	1.00	Clonal	0	1	LOH	1	0
P-0017565-T01-IM5	p.X23_splice	Splice acceptor	0.16	0.12	0.20	Subclonal	No material	0	LOH	1	0
P-0007997-T01-IM5	p.S14Fs*29	Frameshift	NA	NA	NA	NA	100	NA	DIPLOID	2	1
P-0008180-T01-IM5	p.T93Lfs*10	Frameshift	0.99	0.90	1.00	Clonal	30	1	DIPLOID	2	1
P-0017565-T01-IM5	p.M1?	Start lost	0.38	0.34	0.41	Subclonal	No material	0	LOH	1	0
P-0008317-T01-IM5	p.L15Fs*41	Frameshift	NA	NA	NA	NA	0	NA	OTHER	3	NA
P-0008721-T01-IM5	p.A8D	Missense	0.80	0.74	0.85	Clonal	0	1	DIPLOID	2	1
P-0010125-T01-IM5	p.Y46Wfs*8	Frameshift	0.51	0.44	0.59	Subclonal	0	0	DIPLOID	2	1
P-0010125-T01-IM5	p.C45F	Missense	0.63	0.55	0.72	Subclonal	0	0	DIPLOID	2	1
P-0021049-T01-IM6	p.L15Fs*41	Frameshift	1.00	0.96	1.00	Clonal	0	1	LOH	1	0
P-0010308-T01-IM5	p.L15Fs*41	Frameshift	NA	NA	NA	NA	100	NA	DIPLOID	2	1
P-0010798-T01-IM5	p.L15Fs*41	Frameshift	0.86	0.80	0.92	Clonal	0	2	DIPLOID	2	1
P-0010798-T01-IM5	p.V69Wfs*34	Frameshift	0.98	0.92	1.00	Clonal	0	2	DIPLOID	2	1
P-0012402-T01-IM5	p.E89*	Stop gained	NA	NA	NA	NA	0	NA	DIPLOID	2	1
P-0012402-T01-IM5	p.C45G	Missense	NA	NA	NA	NA	0	NA	DIPLOID	2	1
P-0012402-T01-IM5	p.R117*	Stop gained	NA	NA	NA	NA	0	NA	DIPLOID	2	1
P-0013082-T01-IM5	p.S16Afs*27	Frameshift	1.00	0.95	1.00	Clonal	0	2	DIPLOID	2	1
P-0013082-T01-IM5	p.V69Wfs*34	Frameshift	1.00	0.96	1.00	Clonal	0	2	DIPLOID	2	1
P-0013227-T01-IM5	p.G17D	Missense	NA	NA	NA	NA	50	NA	DIPLOID	2	1
P-0013492-T01-IM5	p.Q109*	Stop gained	1.00	0.99	1.00	Clonal	0	2	DIPLOID	2	1
P-0013492-T01-IM5	p.V69Wfs*34	Frameshift	1.00	0.99	1.00	Clonal	0	2	DIPLOID	2	1
P-0004795-T01-IM5	p.S40*	Stop gained	1.00	0.99	1.00	Clonal	No material	1	CNLOH	2	0
P-0014616-T01-IM6	p.T93Lfs*10	Frameshift	0.81	0.74	0.88	Clonal	0	1	DIPLOID	2	1
P-0014616-T01-IM6	p.F82lfs*20	Frameshift	0.37	0.32	0.43	Subclonal	0	1	DIPLOID	2	1

(Continued on following page)

TABLE A1. Predicted *B2M* Mutation Clonality by Cellularity-Corrected Allele Fraction via FACETS and Corresponding Protein Expression (IHC) (Continued)

Sample ID	Protein Change	Mutation Type	CCF	CCF Lower Bound	CCF Upper Bound	Predicted Clonality	B2M Expression (%)	No. of Clonal *B2M* Mutations	FACETS Call	TCN	LCN
P-0014616-T01-IM6	p.L15Ffs*41	Frameshift	0.51	0.45	0.58	Subclonal	0	1	DIPLOID	2	1
P-0014787-T01-IM6	p.L15Ffs*41	Frameshift	0.88	0.81	0.96	Clonal	No material	2	DIPLOID	2	1
P-0014787-T01-IM6	p.S16Afs*27	Frameshift	1.00	0.93	1.00	Clonal	No material	2	DIPLOID	2	1
P-0007882-T01-IM5	p.M1?	Start lost	1.00	0.99	1.00	Clonal	No material	1	CNLOH	2	0
P-0007882-T01-IM5	p.T93Hfs*2	Frameshift	0.59	0.49	0.69	Subclonal	No material	1	CNLOH	2	0
P-0008226-T02-IM5	p.X22_splice	Splice donor	1.00	1.00	1.00	Clonal	0	1	CNLOH	2	0
P-0016560-T01-IM6	p.I21V	Missense	0.79	0.72	0.87	Clonal	No material	1	DIPLOID	2	1
P-0013981-T01-IM5	p.V69Wfs*34	Frameshift	1.00	1.00	1.00	Clonal	0	1	CNLOH	2	0
P-0021393-T01-IM6	p.L15Ffs*41	Frameshift	1.00	0.99	1.00	Clonal	No material	1	CNLOH	2	0
P-0017583-T01-IM5	p.T88*	Frameshift	1.00	0.84	1.00	Clonal	No material	1	DIPLOID	2	1
P-0017925-T01-IM6	p.T93Hfs*2	Frameshift	0.81	0.71	0.93	Clonal	No material	1	DIPLOID	2	1
P-0017986-T01-IM6	p.V69Wfs*34	Frameshift	NA	NA	NA	NA	0	NA	DIPLOID	2	1
P-0017986-T01-IM6	p.T93Hfs*2	Frameshift	NA	NA	NA	NA	0	NA	DIPLOID	2	1
P-0018437-T01-IM6	p.L15Ffs*41	Frameshift	1.00	0.99	1.00	Clonal	No material	1	DIPLOID	2	1
P-0019710-T01-IM6	p.M1?	Start lost	NA	NA	NA	NA	No material	NA	DIPLOID	2	1
P-0020143-T01-IM6	p.S16Afs*27	Frameshift	NA	NA	NA	NA	0	NA	DIPLOID	2	1
P-0020143-T01-IM6	p.V69Wfs*34	Frameshift	NA	NA	NA	NA	0	NA	DIPLOID	2	1
P-0020330-T01-IM6	p.L15Ffs*41	Frameshift	1.00	0.99	1.00	Clonal	No material	2	DIPLOID	2	1
P-0020330-T01-IM6	p.Y46C	Missense	0.86	0.78	0.94	Clonal	No material	2	DIPLOID	2	1
P-0020633-T01-IM6	p.V69Wfs*34	Frameshift	1.00	0.93	1.00	Clonal	0	2	DIPLOID	2	1
P-0020633-T01-IM6	p.L43P	Missense	0.82	0.73	0.91	Clonal	0	2	DIPLOID	2	1
P-0021090-T01-IM6	p.V105A	Missense	NA	NA	NA	NA	0	NA	DIPLOID	2	1
P-0021090-T01-IM6	p.Y30*	Stop gained	NA	NA	NA	NA	0	NA	DIPLOID	2	1
P-0021090-T01-IM6	p.S40*	Stop gained	NA	NA	NA	NA	0	NA	DIPLOID	2	1
P-0021771-T01-IM6	p.X22_splice	Splice donor	0.93	0.82	1.00	Clonal	100	1	DIPLOID	2	1
P-0022111-T01-IM6	p.V69Sfs*21	Frameshift	NA	NA	NA	NA	No material	NA	DIPLOID	2	1

Abbreviations: CCF, cancer-cell fraction; CNLOH, copy neutral loss of heterozygosity; FACETS, Fraction and Allele-Specific Copy Number Estimates from Tumor Sequencing; IHC, immunohistochemistry; LCN, lesser minor copy number; LOH, loss of heterozygosity; NA, CCF could not be calculated because of low tumor purity; TCN, total copy number.

TABLE A2. IHC Expression of Immune and MHC Markers in *B2M*-Mutant Versus WT CRC

Characteristic	*B2M* Mutated (n = 44)	*B2M* WT (n = 26)	P
B2M expression			< .001
Lost	32 (73)	0	
Partially lost	7 (16)	0	
Retained	5 (11)	26 (100)	
MHC class I expression			.64
Lost	14 (31.8)	10 (38.5)	
Retained	30 (68.2)	16 (61.5)	
Average CD3 lymphocytes			.07
Minimum	1.4	0.2	
Maximum	150	150	
Median	22.3	37.3	
Mean	45.6	66.9	
Average CD8 lymphocytes			.5
Minimum	0.2	0	
Maximum	150	150	
Median	15.1	49	
Mean	36.3	58.6	
PD-L1 interface, %			.07
> 20	32 (72.7)	13 (50)	
≤ 20	12 (27.3)	13 (50)	

Abbreviations: CRC, colorectal cancer; IHC, immunohistochemistry; MHC, major histocompatibility; PD-L1, programmed death-1 ligand; WT, wild type.

TABLE A3. Response Data of Patients With *B2M*-Mutant CRC Who Received IOs

CBIO ID	RECIST Response	Immunotherapy Type	MSI Status	B2M Mutations	*B2M* IHC (%)	Treatment Duration (months)	Reason for Stopping	RECIST
P-0010587	PR	PD-1 inhibitor	MSI-H	V69Wfs*34, L15fs*41	0	18.5		−0.8095
P-0005823	PR	PD-L1 inhibitor	MSI-H	p.V69Wfs*34, p.T93Lfs*10	0	5	Surgery (tumor starting to grow)	−0.5903
P-0020431	PR	PD-1 inhibitor	MSI-H	X116_splice	0	18		−0.5225
P-0025883	PR	PD-1 inhibitor	MSI-H	L15fs*41	0	4		−0.48
P-0004051	PR	PD-L1 inhibitor	MSI-H	p.L15Ffs*41, p.T93Hfs*2	No material	3.5	Toxicity (cerebritis)	−0.3393
P-0017697	SD	PD-1 inhibitor	MSI-H	X23_splice, V69Wfs*34	No material	4.5	Toxicity (diarrhea)	−0.2926
P-0015237	SD	PD-1 inhibitor	MSI-H	V69wfs*34, S16Afs*27	0	17		−0.28
P-0021304	SD	PD-1 inhibitor	MSI-H	L15fs*41	No material	1.5	Toxicity (acute interstitial nephritis)	−0.2593
P-0024824	SD	PD-1 inhibitor, targeted therapy	MSS	L107Vfs*7	90	10		−0.1429
P-0029398	SD	PD-1 inhibitor	MSI-H	L10P	0	5		−0.125
P-0016314	SD	PD-1 inhibitor	MSI-H	L13P, L15fs*41	0	2	Progression	−0.0625
P-0011357	PD	PD-L1 inhibitor	MSS*	p.Y87*, p.E64*	0	12	Completed planned treatment	0.6667
P-0007495	No radiologic comparison available	PD-L1 inhibitor	MSS	p.S31*	0	2	Progression	NA

Abbreviations: CRC, colorectal cancer; IHC, immunohistochemistry; IO, immune checkpoint inhibitor; MSI, microsatellite instability; MSI-H, MSI-high; MSS, microsatellite stable; NA, not applicable; PD, progressive disease; PD-1, programmed death-1; PD-L1, PD-1 ligand; PR, partial response; SD, stable disease.